O—H and C—H bond dissociations in non-phenyl and phenyl groups: A DFT study with dispersion and long-range corrections

by Febdian Rusydi

Submission date: 22-Apr-2022 06:09PM (UTC+0800)
Submission ID: 1817171520
File name: 2021rusydi-theo_chem_acco.pdf (1.85M)
Word count: 6307
Character count: 30971

Theoretical Chemistry Accounts (2021) 140:94
https://doi.org/10.1007/s00214-021-02781-6

REGULAR ARTICLE

O—H and C—H bond dissociations in non-phenyl and phenyl groups: A DFT study with dispersion and long-range corrections

Lusia Silfia Pulo Boli[2,3] · Febdian Rusydi[1,2] · Vera Khoirunisa[2,4] · Ira Puspitasari[2,5] · Heni Rachmawati[6,7] · Hermawan Kresno Dipojono[3]

Received: 28 December 2020 / Accepted: 15 May 2021 / Published online: 21 June 2021

Abstract

Hydrogen atom transfer is one important reaction in biological system, in industry, and in atmosphere. The reaction is preluded by hydrogen bond dissociation. To gain a comprehensive understanding on the reaction, it is necessary to investigate how the current computational methods model hydrogen bond dissociation. As a starting point, we utilized density functional theory-based calculations to identify the effect of dispersion and long-range corrections on O—H and C—H dissociations in non-phenyl and phenyl groups. We employed five different methods, namely B3LYP, CAM-B3LYP (with long-range correction), M06-2X, and B3LYP and CAM-B3LYP with the D3 version of Grimme's dispersion. The results showed that for the case of O—H dissociation in two member of phenyl groups, namely phenol and catechol, the dispersion correction's effect was negligible, but the long-range correction's effect was significant. The significant effect was shown by the increasing of energy barrier and the shortening of O—H interatomic distance in the transition state. Therefore, we suggest one should consider the long-range correction in modeling hydrogen bond dissociation in phenolic compounds, namely phenol and catechol.

Keywords Density functional theory · Dispersion correction · Energy · Long-range correction · Non-phenyl and phenyl groups · O—H and C—H dissociations

✉ Febdian Rusydi
rusydi@fst.unair.ac.id

1 Department of Physics, Faculty of Science and Technology, Universitas Airlangga, Jl. Mulyorejo, Surabaya 60115, Indonesia

2 Research Center for Quantum Engineering Design, Faculty of Science and Technology, Universitas Airlangga, Jl. Mulyorejo, Surabaya 60115, Indonesia

3 Department of Engineering Physics, Faculty of Industrial Engineering, Institut Teknologi Bandung, Bandung 40132, Indonesia

4 Engineering Physics Study Program, Institut Teknologi Sumatera, Jl. Terusan Ryacudu, Lampung Selatan 35365, Indonesia

5 Information System Study Program, Faculty of Science and Technology, Universitas Airlangga, Jl. Mulyorejo, Surabaya 60115, Indonesia

6 School of Pharmacy, Institut Teknologi Bandung, Jl. Ganesha 10, Bandung 40132, Indonesia

7 Research Center for Nanoscience and Nanotechnology, Institut Teknologi Bandung, Jl. Ganesha 10, Bandung 40132, Indonesia

1 Introduction

Hydrogen atom transfer is one important reaction that occurs in various environments: the biological systems, the atmosphere, and the industry. In biological systems, the reaction takes place in lipid peroxidation formation [1, 2] and its prevention, [3–8] as well as in free radicals formation [9]. In the atmosphere, the reaction involves hydroxyl radical (OH) and organic or inorganic materials [10, 11]. Meanwhile in industry, one way the reaction occurs is in the presence of a catalyst [12, 13]. Overall, the reaction has been a subject of experimental and computational studies. However, there is still a need to understand how the current computational methods can model hydrogen bond dissociation. This understanding will help to achieve a comprehensive insight into the hydrogen atom transfer reaction.

Numerous publications have reported the usage of computational methods based on density functional theory (DFT) to investigate hydrogen bond dissociation. One quantity describing the hydrogen bond dissociation is bond dissociation energy (BDE). In 1999, Barckholtz et al. reported the use of one DFT exchange-correlation (XC) functional,

B3LYP, to predict C-H BDE of small aromatics. The predictions were in agreement with the available experimental values [14]. In the following years, the XC was used to predict the BDE of various bonds in small and large molecules [15–17]. On the other hand, other publications showed that B3LYP has low accuracy [18–20] but is reliable to predict the substituent effect such as in alkyl and peroxyl radicals [18]. In 2008, Zhao and Truhlar introduced XC from the Minnesota family, M06-2X. This XC has much-improved accuracy in predicting BDE [21]. M06-2X is reliable for various cases, such as predicting substituent effects on O-C and C-C BDE of lignin [22] and predicting BDE of polyphenols in various solvents [23]. The DFT used for the above prediction was unrestricted [15, 22]. In addition to B3LYP and M06-2X, Du et al. used CAM-B3LYP, which includes a long-range correction to B3LYP, in their calculations. They found that CAM-B3LYP underestimates O-CH3 BDE relative to experimental values. However, this XC has better performance for aromatic molecules than for non-aromatic molecules [24]. Even though many references have reported the use of various DFT XCs for predicting BDE, there is still limited references reported about the path taken by hydrogen atom during the bond dissociation. The use of XCs to model the path is necessary to gain insight into the hydrogen atom transfer reactions. Thus, the present work investigates the effect of dispersion and long-range corrections in O-H and C-H bond dissociations. The corrections have been integrated into DFT XCs. Therefore, it is necessary to use DFT to identify the effect of dispersion and long-range correction on O-H and C-H bond dissociations.

This work aims to study the effects of dispersion and long-range corrections on the O-H and C-H bond dissociations computationally. We utilize DFT with three functionals combined with the D3 version of Grimme's dispersion. The combination is five methods: B3LYP that has been used for chemical computation, CAM-B3LYP that includes a long-range correction, B3LYP-GD3 and CAM-B3LYP-GD3 which include Grimme's dispersion, and M06-2X that has a good performance for noncovalent interactions [25–28]. The dissociation is designed to occur at O-H and C-H bonds of six non-phenyl and three phenyl groups. The phenyl groups containing O-H bonds are chosen to represent the phenolic compounds. To achieve the goal, we calculate bond dissociation energy and build hydrogen bond dissociation pathways using two techniques: a relaxed scan calculation and a geometry optimization in the ground and transition states. We have used these two techniques to study other chemical reactions [29–32]. This study will answer the following question: What are the effects of the dispersion and long-range corrections on the O-H and C-H dissociations of non-phenyl and phenyl groups?

2 Computational models

2.1 Reaction model

Scheme 1 presents our model for the homolytic hydrogen bond dissociation. The reactant was R-H′ possessing O-H, or C-H, bond; the products were R· and a hydrogen atom (H′·). There were nine molecules of interest for R-H′, which were (a) hydroxyl, (b) methylidyne, (c) water, (d) methane, (e) methanol, (f) ethane, (g) toluene, (h) phenol, and (i) catechol.

$$\underset{[\text{in.}]}{R{-}H'} \longrightarrow \underset{[\text{fi.}]}{R^{\bullet} + H'^{\bullet}}$$

Scheme 1 The initial state [in.] and the final state [fi.] of the reaction model.

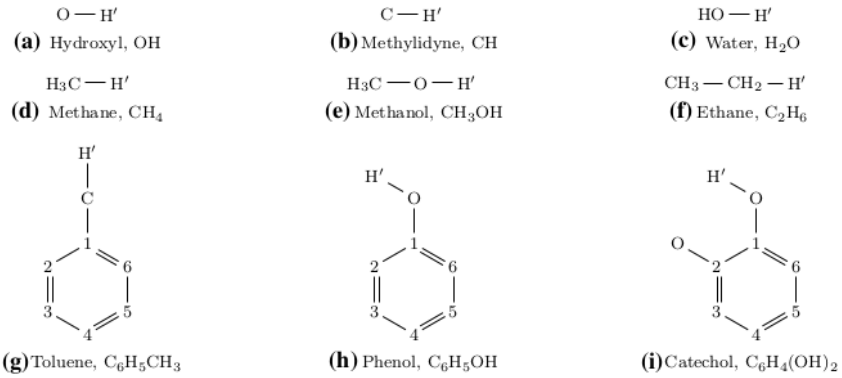

Fig. 1 Kekulé structures of the molecules of interest. The primed H was the dissociated hydrogen atom. For clarity in molecules (g)–(i), only dissociated hydrogen atom was shown, and carbon atoms were replaced by numbers

Table 1 List of methods used in the manuscript

M1	B3LYP
M2	B3LYP + GD3
M3	CAM-B3LYP
M4	CAM-B3LYP + GD3
M5	M06-2X

Figure 1 presents the Kekulé structures of these molecules.

2.2 DFT calculations

We performed computational techniques with the basis of DFT [33, 34]. We used 6-311++G(d,p) basis set with three different XCs; they were (1) B3LYP, (2) CAM-B3LYP, and (3) M06-2X which were implemented in Gaussian 16 software [35]. The first XC has become a standard functional for a geometry structure study, while the second XC has improved the long-range interaction of the first XC. The third XC has been parameterized, such that noncovalent interactions take into account. We applied the D3 version of Grimme's dispersion to accommodate the dispersion effect along the dissociation pathways. We combined the XCs and the dispersion into five different methods, as shown in Table 1. In addition to DFT, we used Natural Bond Orbital (NBO) calculations for the natural hybrid orbital and charge population analysis [36].

The procedure for DFT calculations is as follows. First, we validated that the three XCs were capable to obtain the spin-state and the geometry in the ground state. For this purpose, we chose hydroxyl and phenol because they represented molecules with odd and even number of electrons and because their experimental results were available. Second, we performed a geometry optimization to obtain the geometry of all molecules of interest in the ground state using the five calculation methods. To obtain BDE ($D°$) of hydrogen, we coupled DFT with frequency calculations. It resulted in the total electronic energy with thermal correction to enthalpy at 298.15 K in the ground state. $D°$ was the enthalpy difference between the final and the initial states in Scheme 1. Third, we constructed the hydrogen bond dissociation pathways.

We employed two different computational techniques for the third DFT calculations procedure. The first technique was a relaxed scan calculation, where one hydrogen atom (with prime mark in Figure 1) left oxygen or carbon atom of R· and let R· relaxed. The increments were set to be 0.2 Å for all methods. The second one was based on the geometry optimization in the ground and transition states. We applied the first technique to the selected non-phenyl and phenyl groups. The value of $D°$ that was affected and was not affected by dispersion and/or long-range corrections became the restriction in selecting molecules in the first technique. The first technique resulted in potential energy curve (PEC), and the dissociation pathway was visualized using a polar coordinate. We emphasized that the pathway that led to other than hydrogen bond dissociation would not be discussed further. The PEC that was affected by dispersion and/or long-range corrections became the restriction to select molecules in the second technique. The second technique yielded a dissociation pathway in energy level diagrams (ELD). We have successfully applied both techniques in our previous studies for bigger molecules [29–32].

We excluded PEC results from M06-2X in the current study because it produced unreasonable results. We also noted that Mardirossian and Head-Gordon [37] reported a similar case. They highlighted that M06-2X poorly predicted the bond length of krypton dimer and benzene-silane dimer through their potential energy curves. We listed the symbols and acronyms in Table 2 to assist readers in getting familiar with them.

3 Results and discussion

3.1 The ground state structures

Spin-state and geometry The geometry optimization using the three XCs obtained the doublet and singlet as the lowest in energy level for hydroxyl and phenol, respectively. On average, the doublet was 4.6 eV lower than the quartet (in hydroxyl), while the singlet was 4.2 eV lower than the triplet (in phenol). The doublet and the singlet were more stable compared to the quartet and the triplet. The results agree with the ground spin-states of hydroxyl and phenol reported in references [38, 39]. Furthermore, the selected geometrical parameters of hydroxyl and phenol in those spin-states were less than 0.017 Å and 1.4 degrees (see Table 3). The values were within the accuracy limit for DFT calculations [40].

Table 2 List of symbols and acronyms used throughout the manuscript

Symbol/acronym	Description
$D°$	Bond dissociation energy
r13	Distances between atoms
BDE	Bond dissociation energy
DFT	Density functional theory
ELD	Energy level diagram
IS	Intermediate state
NBO	Natural Bond Orbital
PEC	Potential energy curve
TS	Transition state
XC	Exchange-correlation

Table 3 The discrepancy of calculated geometrical parameters of hydroxyl and phenol by (1) B3LYP, (2) CAM-B3LYP, and (3) M06-2X with respect to the experimental values [41]. The parameters were bond length (R, in Å) and bond angle (A, in degree). The parameter in (i) belongs to hydroxyl, while others belong to phenol

	Parameter	Expr.	(1)	(2)	(3)
(i)	R(O,H′)	0.970	+0.006	+0.005	+0.003
(ii)	R(O,H′)	0.956	+0.007	+0.005	+0.005
(iii)	R(C,C)av	1.397	− 0.003	− 0.009	-0.006
(iv)	R(1,O)	1.364	+0.006	0.000	− 0.001
(v)	R(4,H)	1.082	+0.001	+0.001	0.000
(vi)	R(5,H)	1.076	+0.008	+0.008	+0.008
(vii)	R(6,H)	1.084	+0.002	+0.001	+0.002
(viii)	A(1,O,H′)	109.0	+0.8	+1.0	+0.8

Therefore, the three XCs were capable to obtain the correct ground state structure of the molecules with odd or even number of electrons. Based on these results, the same XCs were used to obtain the ground spin-state of other molecules with an odd and even numbers of electrons which were doublet and singlet, respectively.

The dispersion and long-range corrections Table 4 presents O-H′ and C-H′ bond lengths of the obtained ground state geometry of all molecules of interest. The Cartesian coordinates of the ground state geometry were given in Table S1-S9 of Supplementary Information (SI). Calculation using the method with dispersion correction (M2 and M4) obtained the same bond length as the method without the correction (M1 and M3). The method with the long-range correction (M3) and the method parameterized with dispersion-like interaction (M5) obtained slightly shorter bond lengths (the negative values) than the method without the correction (M1). The results suggest the dispersion and the long-range corrections do not alter the ground state O-H′ and C-H′ bond lengths of our molecules of interest.

3.2 The bond dissociation energy

Table 5 presents the discrepancy of $D°$ between the calculated and experimental values. Among all methods, the M5 method obtained $D°$ the closest to the experimental values for molecules with singlet spin-state. The results supported the work of Zhao and Truhlar [21], which suggested using the M5 method for $D°$ calculations of molecules with singlet spin-state. Therefore, M06-2X functional is suitable for dealing with the hydrogen bond dissociation energy of molecules with singlet spin-state.

The discrepancies obtained by M2, M3, and M4 were varied compared to that obtained by M1. In all molecules

Table 4 The difference of calculated O-H′ and C-H′ bond lengths from M1 (Å). The label referred to Fig. 1

	Molecule	Bond	M1	M2	M3	M4	M5
(a)	Hydroxyl	O-H′	0.976	0.000	−0.002	−0.002	−0.004
(b)	Methylidyne	C-H′	1.127	0.000	−0.003	−0.003	−0.007
(c)	Water	O-H′	0.962	0.000	−0.001	−0.001	−0.003
(d)	Methane	C-H′	1.091	0.000	−0.001	−0.001	−0.002
(e)	Methanol	O-H′	0.961	0.000	−0.002	−0.002	−0.003
(f)	Ethane	C-H′	1.094	0.000	−0.001	−0.001	−0.002
(g)	Toluene	C-H′	1.094	0.000	−0.002	−0.002	−0.002
(h)	Phenol	O-H′	0.963	0.000	−0.002	−0.002	−0.002
(i)	Catechol	O-H′	0.962	0.000	−0.002	−0.002	−0.002

Table 5 The discrepancy of calculated $D°$ with respect to the experimental values (kJ/mol) [41, 42]. The label referred to Fig. 1

	Molecule	Bond	Expr.	M1	M2	M3	M4	M5
(a)	Hydroxyl	O-H′	429.73	−1.1	−1.1	−0.8	−0.8	−9.2
(b)	Methylidyne	C-H′	338.4	+1.8	+1.8	−2.2	−2.2	−8.1
(c)	Water	O-H′	497.32	−17.1	−17.1	−14.0	−14.0	−11.7
(d)	Methane	C-H′	439.3	−8.3	−8.2	−7.1	−7.0	−6.1
(e)	Methanol	O-H′	440.2	−26.4	−25.2	−21.1	−20.3	−11.5
(f)	Ethane	C-H′	420.5	−8.9	−7.6	−6.8	−6.0	−3.4
(g)	Toluene	C-H′	375.5	−10.8	−9.1	−5.8	−4.7	+2.9
(h)	Phenol	O-H′	362.8	−16.0	−14.6	−9.6	−8.6	+6.7
(i)	Catechol	O-H′	342.3	−32.0	−29.9	−24.0	−22.5	−9.8

[Table 5 (a)-(i)], M2 obtained 0.9 kJ/mol (in average) discrepancies higher than M1 did. Moreover, M4 obtained 0.6 kJ/mol (in average) discrepancies higher than M3 did. The results indicate that the dispersion correction does not alter the calculated $D°$ of molecules with singlet and doublet spin-states. In hydroxyl and methylidyne [Table 5 (a) and (b)], M3 obtained 1.9 kJ/mol (in average) discrepancies lower than M1 did. Meanwhile, in other molecules [Table 5 (c)-(i)], M3 obtained 4.4 kJ/mol (in average) discrepancies higher than M1 did. The 4.4 kJ/mol is significant, which implies that the long-range correction is the reason for $D°$ alteration of molecules with singlet spin-state. Thus, the long-range correction plays a role in altering $D°$ of molecules with singlet spin-state but not the molecules with doublet spin-state.

Among seven molecules in Table 5 (c)-(i), the alteration of discrepancies from M1 to M3 on O-H′ bonds differed from that on C-H′ bonds. The seven molecules were in their singlet spin-state. For four molecules with O-H′ bonds, the discrepancies increased by 5.7 kJ/mol (on average) from M1 to M3. However, for three molecules with C-H′ bonds, the discrepancies only increased by 2.8 kJ/mol (in average) from M1 to M3. The increase on O-H′ bonds is more significant than on C-H′ bonds. It indicates that the long-range correction alters the calculated $D°$ on O-H′ bond more than that on C-H′ bond of molecules with singlet spin-state.

The increase in the discrepancy on O-H′ bonds was not accompanied by bond length alteration but by O-H′ bond orbitals alteration. As discussed in Sect. 3.1, from M1 to M3, the ground state O-H′ bond length only altered by 0.002 Å. However, from M1 to M3, the O-H′ bond orbitals altered mainly in $(sp^{\lambda})_O$ hybrid orbitals (see Table S10 of the SI). According to the NBO calculations, the average percentage of alteration at $(sp^{\lambda})_O$ hybrid orbitals was 33 times more than that at $(sp^{\lambda})_C$ hybrid orbitals. Therefore, the long-range correction plays a role in altering the electron density in the O-H′ bond orbitals; hence the calculated $D°$ of O-H′ bond increases.

3.3 The potential energy curve

Figure 2 shows the PECs of four selected molecules together with their respective polar coordinates. All methods yielded two types of PEC profiles. The first type was a PEC-like of dissociation diatomic molecules [Fig. 2(a)–2(b) left]. Region I described the dissociation process, and region II described H′· was already a free atom. All methods agreed one to each other. The second type was somewhat challenging to explain since not all methods agreed [Fig. 2(c)–2(d) left]. There was region III that contained barriers. PEC profiles in methylidyne and ethane were supportive results to the first type, while PEC profiles in hydroxyl and water were supportive results to the second type. Hence, they were placed in Supporting Information [Figure S1(a)–(b) and S1(c)–(d) left]. On the other hand, the polar coordinates show that the hydrogen bond dissociation pathways in methane [Fig. 2(a) right] are different from those in other molecules [Fig. 2(b)–2(d) right and Figure S1(c)–(d) right of the SI]. All methods were only agreed for methane. It implies that the corrections (long-range and dispersion) significantly affect the pathway in real space rather than in the PEC profile.

Overall, the PEC profiles of methanol and phenol [Fig. 2(c)–2(d) left] were explained as follows. In region III, methanol and phenol had barriers; methanol had one, and phenol had at least three barriers. In both cases, M2 yielded a similar barrier height to M1 did. So did M4 and M3. It means the dispersion correction does not alter the PEC profile of O-H′ dissociation. However, in both cases, M3 yielded a different barrier height than M1 did. The results indicate that the long-range correction does alter the PEC profile of O-H′ dissociation. Therefore, the long-range correction plays a more significant role than the dispersion correction in the PEC profiles of O-H′ dissociation.

In detail, for phenol [Fig. 2(d)], the variation of PEC profiles was accompanied by the variation of dissociation pathways in the polar coordinate. Both variations occurred only at a certain O-H′ distance ($r_{O–H'}$) range. The PEC profile variation range was around 1.8–3 Å; while the pathway variation range was around 2–4 Å. In those ranges, M3 yielded a different profile and pathway than M1 did. Kamiya et al. [43] also obtained different profiles when using XCs with long-range correction in a system interacting through a van der Waals interaction (noncovalent interaction). Thus, the different profiles obtained by the long-range correction (M3) may be due to the presence of noncovalent interactions, particularly at a region with barriers. Therefore, in line with its role in O-H′ BDE, the long-range correction may play a role in the energy barrier of O-H′ dissociation.

Along the phenol dissociation pathway, M1 and M3 obtained different r at B1a, B1b, and B2 (See Table S11 of the SI). At B1a and B1b, atom H′· was located around atom O [See Figure S2 of the SI]. Here, M3 obtained shorter $r_{O–H'}$ at B1a than M1 did at B1b. Different than at B1a and B1b, at B2 atom H′· was located between atom 2 and atom 3. Here, M3 obtained shorter $r_{2–H'}$ and longer $r_{3–H'}$ than M1 did. The results indicate that the shortening and lengthening of r are due to the long-range correction.

The r alteration after the introduction of long-range correction was accompanied by atomic charges alteration. The NBO calculations showed that atom O, 2, and 3 [See Fig. 1(h)] were negatively charged while atom H′· was positively charged. At B1a, M3 yielded greater positive charge on atom H′· and greater negative charge on atom O than M1 did. It implies that the increasing coulombic attraction between atom O and H′· is the reason for the shortening of $r_{O–H'}$ at B1a. At B2, M3 obtained lesser positive charge on

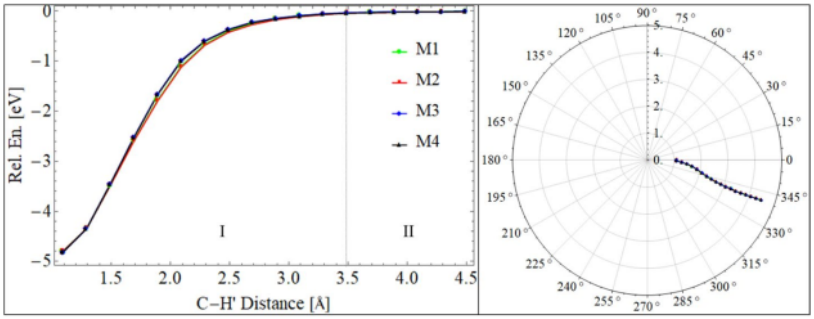

(a) PEC (left) and polar coordinate (right) of methane.

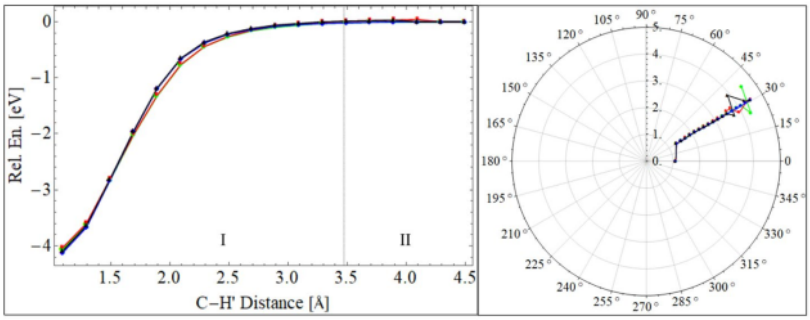

(b) PEC (left) and polar coordinate (right) of toluene.

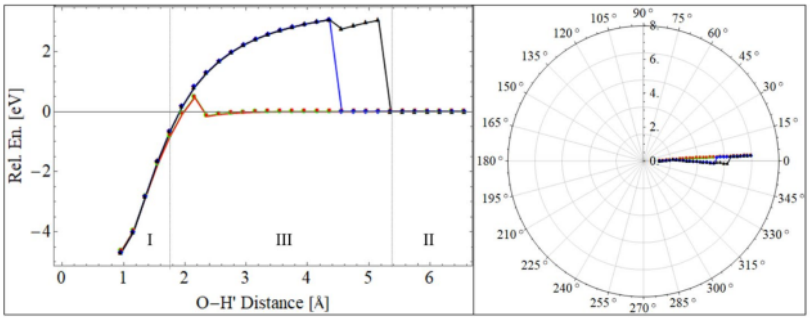

(c) PEC (left) and polar coordinate (right) of methanol.

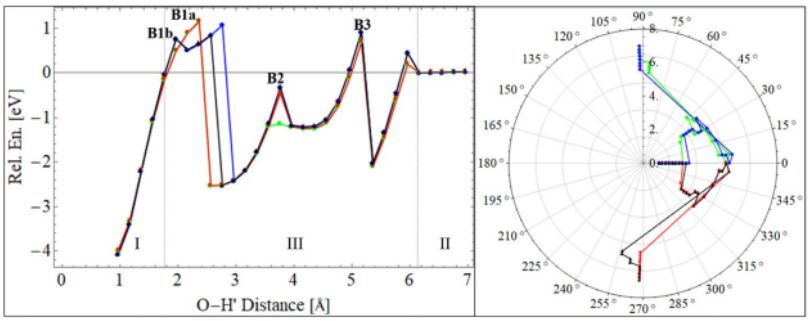

(d) PEC (left) and polar coordinate (right) of phenol.

Fig. 2 PECs of C-H′ and O-H′ bond dissociations with their respective polar coordinates. The I, II, and III represented three different regions based on the similarity of events at each region. Angles in the polar coordinate were H-C-H′ in methane, 2–1–C-H′ in toluene, H-C-O-H′ in methanol, and 2–1–O-H′ in phenol (see Fig. 1). The initial angle was at zero degree, then deviated clockwise or counterclockwise. Particularly in methane, the clockwise represented inward deviation. **B1a**, **B1b**, **B2**, and **B3** in (d) represented first barrier obtained by M1 and M2, first barrier obtained by M3 and M4, second and third barrier obtained by all four methods, respectively

atom H′· and greater negative charge on atom 2 than M1 did. It indicates that the increasing coulombic attraction between atom 2 and H′· is the reason for the shortening of the $r_{2–H'·}$ At this location, M3 obtained lesser negative charge on atom 3 than M1 did. It implies the increasing coulombic repulsion between atom 3 and H′· is the reason for the lengthening of the $r_{3–H'·}$ Therefore, the Coulombic interactions play a role in the alteration of r.

3.4 The dissociation pathway

Figure 3 shows the O-H′ dissociation pathways of two selected molecules, phenol and catechol, in an ELD. For the case of phenol [Fig. 3(a)], each pathway had three transition states (TS) and three intermediate states (IS) as predicted earlier in Fig. 2(d)left; while for the case of catechol [Fig. 3(b)], each pathway had two TSs and two ISs. The experiment has observed the presence of IS1 in a photochemical reaction [44]. While a theoretical study reported IS1 and IS3 as two isomers of phenol [45]. Another theoretical study reported the first step in decomposition of catechol lead to IS4 [46]. The similarity between the molecules in the intermediate states with the previous studies indicates the possibility of hydrogen migration before O-H′ dissociation occurred.

The dissociation pathways in phenol and catechol showed that all methods obtained the same relative electronic energy order in each TS. The order for both cases was M1 ≈ M2 < M3 ≈ M4 < M5. For the case of phenol, the average difference between the energy obtained by methods with long-range correction (M3 and M4) and methods without the correction (M1 and M2) was 0.16 eV. Similarly, for the case of catechol, the average difference was 0.14 eV. The differences are significant. It was aligned with the PEC profile difference [Fig. 2(d)left] after the long-range correction

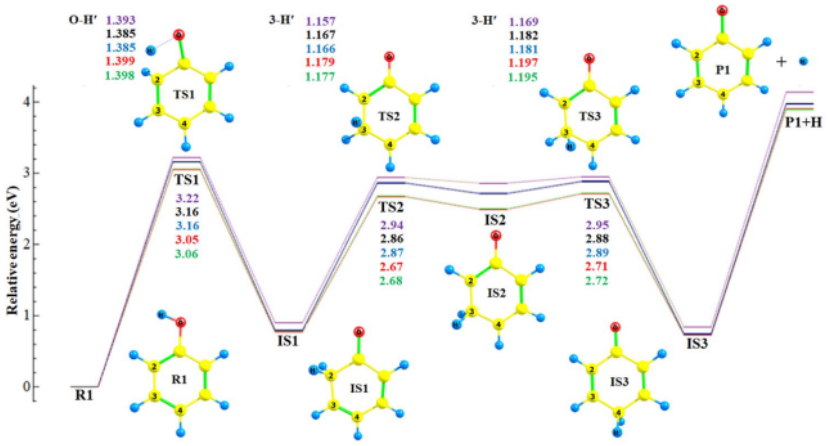

(a) O−H′ dissociation pathways of phenol

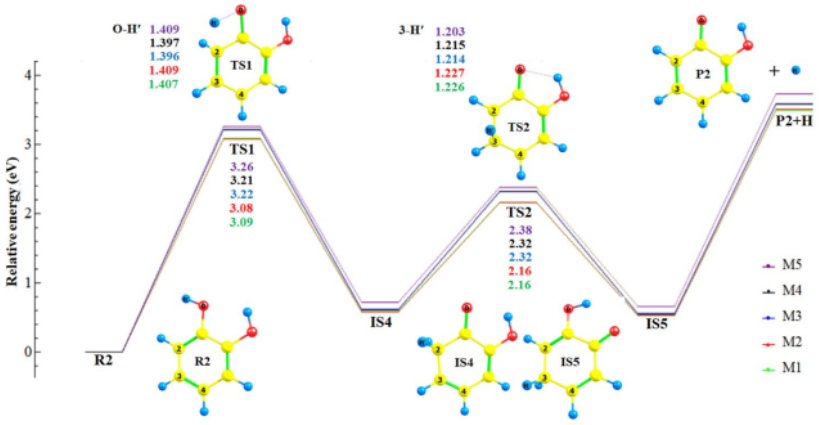

(b) O−H′ dissociation pathways of catechol

Fig. 3 Energy level diagram for O-H′ dissociation pathways of two selected molecules. R1, R2, P1, and P2 represent phenol, catechol, product of phenol dissociation, and product of catechol dissociation. While TS and IS stand for transition state and intermediate state. The TSs were shown with the selected interatomic distances (unit in Å)

was introduced, particularly at the region with barriers. The results imply that the long-range correction predicts the dissociation is more difficult at a region where the noncovalent interaction may be present. Therefore, the correction indeed plays a role in the energy barrier of O-H′ dissociation.

Methods with long-range correction (M3 and M4) obtained shorter r than methods without the correction did in the TS structures. For the case of phenol, the $r_{O–H'}$ and $r_{3–H'}$ shortened by 0.01 Å on average. The shortening was also similar to the case of catechol. The 0.01 Å is significant compared to the O-H′ bond length shortening in the ground state of phenol and catechol [Table 4(h) and (i)]. Thus, the shortening confirms the shortening of r along the dissociation pathway discussed in Subsection 3.3. For this reason, the long-range correction indeed plays a role in r in the transition state.

Methods with the long-range correction (M3 and M4) obtained similar relative electronic energy to M5 did in the TSs. The average differences of relative electronic energy obtained by those methods were 0.07 for phenol and 0.06 for catechol. These values are very small which indicate the similarity of transition state according to those methods. Therefore, CAM-B3LYP and M06-2X predict comparable transition state of O-H′ dissociation.

Overall, all methods showed consistent performances on the BDE calculations and O-H′ dissociation pathways prediction. For the BDE calculations, the methods obtained the $D°$ of O-H′ bonds in all molecules increased in the following order: M1 ≈ M2 < M3 ≈ M4 < M5. The increase of $D°$ after the presence of long-range correction in CAM-B3LYP (M3) was in agreement with the study by Chan et al. [47] For the pathways prediction, the methods obtained variation of pathways in phenol and catechol dissociation. The variations were identified by the alteration in energy barriers and $r_{O–H'}$ in the TS. The energy barrier increased in the same order as the increase in $D°$ of O-H′ bonds. This result validates the study by Peach et al. [48] that showed increasing barrier height when using CAM-B3LYP compared to B3LYP. The increasing energy barriers was accompanied by the shortening of $r_{O–H'}$ as follows: M1 ≈ M2 > M3 ≈ M4. The shortening due to the long-range correction (M3) was in agreement with our previous study [31]. The results show the significance of this research: the use of long-range correction in CAM-B3LYP affects the $r_{O–H'}$ in TS. On the other hand, the M06-2X used in this study predicted the highest $D°$ and energy barrier. The $D°$ was similar to the experimental observation. Its developer suggested the functional for applications involving main group thermochemistry, kinetics, and noncovalent interactions [21, 28].

4 Conclusion

We have studied the effects of dispersion and long-range corrections on O-H and C-H dissociations of non-phenyl and phenyl groups. The effects were identified through bond dissociation energy and dissociation pathways. We summarized that the dispersion correction had negligible effects on the O-H and C-H bond dissociation energies and the non-phenyl and phenyl groups dissociation pathways. While the long-range correction in CAM-B3LYP had a minor effect on the O-H bond dissociation energy and a significant effect on the O-H dissociation pathways. We found that the long-range correction increased the bond dissociation energy of the O-H bond of non-phenyl and phenyl groups in their singlet states by 5.7 kJ/mol. We argued that the increase was due to the alteration of electron density in the O-H bond orbitals. However, the dissociation energy was still far from the experimental results. The significant effects of the long-range correction on the O-H dissociation pathways occurred in two members of phenyl groups, namely phenol and catechol. The effects were identified as follows. First, the correction shortened the O-H distances in the transition states by 0.01 Å, on average. Second, the correction increased the energy barrier by 0.16 eV (in phenol) and 0.14 eV (in catechol), on average. Overall, our results support other theoretical studies on the increasing energy barrier due to the long-range correction. Accordingly, we suggest that one should consider the long-range correction when studying hydrogen bond dissociation in phenolic compounds, such as phenol and catechol.

Supplementary Information The online version contains supplementary material available at https://doi.org/10.1007/s00214-021-02781-6.

Acknowledgements Authors thank to Rizka Nur Fadilla (Universitas Airlangga, Indonesia) and Prof. Azizan Ahmad (University Kebangsaan Malaysia, Malaysia) for the insightful discussions. LSPB is grateful for the doctoral scholarship by Lembaga Pengelola Dana Pendidikan (LPDP). All calculations using Gaussian 16 software are performed at Riven Cluster, the high-performance computing facility in Research Center for Quantum Engineering Design, Universitas Airlangga, Indonesia.

Author Contributions F.R. contributed to conceptualization; L.S.P.B, H.R., and I.P. contributed to formal analysis; L.S.P.B and V.K. were involved in investigation; F.R. and L.S.P.B contributed to methodology; I.P. provided the resources; L.S.P.B contributed to writing—original draft preparation; F.R. and H.K.D contributed to writing—review and editing. All authors have read and agreed to the published version of the manuscript.

Declarations

Funding This work was supported by Universitas Airlangga under grant scheme Riset Kolaborasi Mitra Luar Negeri 2019 no. 1148/UN3.14/LT/2019 and by Direktorat Riset dan Pengabdian Masyarakat, Deputi Bidang Penguatan Riset dan Pengembangan Kementerian Riset dan Teknologi/Badan Riset dan Inovasi Nasional, Republik Indone-

sia under grant scheme Penelitian Dasar Unggulan Perguruan Tinggi (PDUPT) 2020 no. 1288r/I1.C06/PL/2020.

Conflict of Interest The authors have no conflicts of interest to declare that are relevant to the content of this article.

Availability of Data and Materials All data analyzed during this study are included in this published article and its supplementary information file.

Code Availability Not Applicable.

References

1. Zielinski ZAM, Pratt DA (2017) J Org Chem 82(6):2817–2825
2. Yin H, Porter NA (2011) Chem Rev 111(10):5944–5972
3. Shang Y, Zhou H, Li X, Zhou J, Chen K (2019) New J Chem 43:15736–15742
4. Vo QV, Nam PC, Bay MV, Thong NM, Cuong ND, Mechler A (2018) Sci Rep 8:12361
5. Xue Y, Zheng Y, An L, Dou Y, Liu Y (2014) Food Chem 151:198–206
6. Iuga C, Alvarez-Idaboy JR, Russo N (2012) J Org Chem 12:3868–3877
7. Galano A, Alvarez-Diduk R, Ramirez-Silva MT, Alarcon-Angeles G, Rojas-Hernandez A (2009) Chem Phys 363:13–23
8. Jovanovic SV, Steenken S, Boone CW, Simic MG (1999) J Am Chem Soc 121:9677–9681
9. Wang Y-N, Eriksson LA (2001) Theor Chem Acc 106:158–162
10. Mallick S, Sarkar S, Bandyopadhyay B, Kumar P (2018) J Phys Chem A 122(1):350–363
11. Kumar M, Sinha A, Francisco JS (2016) Acc Chem Res 49(5):877–883
12. Liang F, Zhong W, Xiang L, Mao L, Xu Q, Kirk SR, Yin D (2019) J Catal 378:256–269
13. Asgari P, Hua Y, Bokka A, Thiamsiri C, Prasitwatcharakorn W, Karedath A, Chen X, Sardar S, Yum K, Leem G, Pierce BS, Nam K, Gao J, Jeon J (2019) Nat Catal 2:164–173
14. Barckholtz C, Barckholtz TA, Hadad CM (1999) J Am Chem Soc 121(3):491–500
15. Wang L, Yang F, Zhao X, Li Y (2019) Food Chem 275:339–345
16. Nantasenamat C, Isarankura-Na-Ayudhya C, Naenna T, Prachayasittikul V (2008) J Mol Graph Model 27:188–196
17. Zhang H-Y, Sun Y-M, Wang X-L (2003) Chem Eur J 9:502–508
18. Brinck T, Lee H-N, Jonsson M (1999) J Phys Chem 103:7094–7104
19. Izgorodina EI, Coote ML, Radom L (2005) J Phys Chem A 109:7558–7566
20. Izgorodina EI, Brittain DRB, Hodgson JL, Krenske EH, Lin CY, Namazian M, Coote ML (2007) J Phys Chem A 111:10754–10768
21. Zhao Y, Truhlar DG (2008) J Phys Chem A 112:1095–1099
22. Beste A, Buchanan AC III (2009) J Org Chem 74(7):2837–2841
23. Zheng Y-Z, Fu Z-M, Deng G, Guo R, Chen D-F (2020) Phytochemistry 178:112454
24. Du T, Quina FH, Tunega D, Zhang J, Aquino AJA (2020) Theor Chem Acc 139:75
25. Yanai T, Tew DP, Handy NC (2004) Chem Phys Lett 393:51–57
26. Grimme S, Antony J, Ehrlich S, Krieg H (2010) J Chem Phys 132:154104
27. Becke AD (1993) J Chem Phys 98:5648
28. Zhao Y, Truhlar DG (2008) Theor Chem Acc 120:215–241
29. Rusydi F, Madinah R, Puspitasari I, Mark-Lee WF, Ahmad A, Rusydi A (2020). Biochem Mol Biol Educ. https://doi.org/10.1002/bmb.21433
30. Fadilla RN, Rusydi F, Aisyah ND, Khoirunisa V, Dipojono HK, Ahmad F, Mudasir, Puspitasari I (2020) Molecules 25: 670
31. Rusydi F, Aisyah ND, Fadilla RN, Dipojono HK, Ahmad F, Mudasir, Puspitasari I, Rusydi A (2019) Heliyon 5: e02409
32. Fadilla RN, Aisyah ND, Dipojono HK, Rusydi F (2017) Procedia Eng 170:113–118
33. Hohenberg P, Kohn W (1964) Phys Rev 136:B864
34. Kohn W, Sham LJ (1965) Phys Rev 140:A1133
35. Frisch MJ, Trucks GW, Schlegel HB,Scuseria GE, Robb MA, Cheeseman JR, Scalmani G, Barone V,Petersson GA, Nakatsuji H, Li X, Caricato M, Marenich AV,Bloino J, Janesko BG, Gomperts R, Mennucci B, Hratchian HP, Ortiz JV, Izmaylov AF, Sonnenberg JL, Williams-Young D,Ding F, Lipparini F, Egidi F, Goings J, Peng B, Petrone A,Henderson T, Ranasinghe D, Zakrzewski VG, Gao J, Rega N, Zheng, Liang W, Hada M, Ehara M, Toyota K, Fukuda R,Hasegawa J, Ishida M, Nakajima T, Honda Y, Kitao O, Nakai H,Vreven T, Throssell K, Montgomery JA, Jr., Peralta J E,Ogliaro F, Bearpark MJ, Heyd JJ, Brothers EN, Kudin K N, Staroverov VN, Keith TA, Kobayashi R, Normand J, Raghavachari K, Rendell AP, Burant JC, Iyengar SS, Tomasi J, Cossi M, Millam JM, Klene M, Adamo C, Cammi R, Ochterski JW, Martin RL, Morokuma K, Farkas O, Foresman JB, Fox DJ (2013) Gaussian 16, Revision C.01, Gaussian, Inc., Wallingford CT
36. Glendening ED, Reed AE, Carpenter JE, Weinhold F Nbo version 3.1
37. Mardirossian N, Head-Gordon M (2016) J Chem Theory Comput 12:4303–4325
38. Jones DB, da Silva GB, Neves RFC, Duque HV, Chiari L, de Oliveira EM, Lopes MCA, da Costa RF, Varella MTN, Bettega MHF, Lima MAP, Brunger MJ (2014) J Chem Phys 141:074314
39. Huber KP, Herzberg G (1979) Molecular spectra and moelcular structure IV constants of diatomic molecules. Springer, US, p 508
40. Young DC, Computational chemistry: A practical guide for applying techniques to real-world problems. Wiley, New York, 2001, Chp. 16, Page 138
41. Haynes WM (2014) CRC Handbook of Chemistry and Physics, 95th ed., CRC Press, Boca Rotan, Chp.9
42. Lucarini M, Pedulli GF, Guerra M (2004) Chem Eur J 10:933–939
43. Kamiya M, Tsuneda T, Hirao K (2002) J Chem Phys 117:6010
44. Parker K, Davis SR (1999) J Am Chem Soc 121:4271–4277
45. Zhu L, Bozzelli JW (2003) J Phys Chem A 107:3696–3703
46. Altarawneh M, Dlugogorski BZ, Kennedy EM, Mackie J (2010) J Phys Chem A 114:1060–1067
47. Chan B, Morris M, Radom L (2011) Aust J Chem 64:394–402
48. Peach MJG, Helgaker T, Salek P, Keal TW, Lutnæs OB, Tozer DJ, Handyd NC (2006) Phys Chem Chem Phys 8:558–562

O—H and C—H bond dissociations in non-phenyl and phenyl groups: A DFT study with dispersion and long-range corrections

ORIGINALITY REPORT

15%	8%	15%	3%
SIMILARITY INDEX	INTERNET SOURCES	PUBLICATIONS	STUDENT PAPERS

PRIMARY SOURCES

1	Vera Khoirunisa, Febdian Rusydi, Lusia S. P. Boli, Ira Puspitasari, Heni Rachmawati, Hermawan K. Dipojono. "The significance of long-range correction to the hydroperoxyl radical-scavenging reaction of trans-resveratrol and gnetin C", Royal Society Open Science, 2021 Publication	4%
2	jurnal.ugm.ac.id Internet Source	1%
3	www.thieme-connect.com Internet Source	1%
4	repository.unair.ac.id Internet Source	1%
5	Febdian Rusydi, Roichatul Madinah, Ira Puspitasari, Wun F. Mark - Lee, Azizan Ahmad, Andrivo Rusydi. "Teaching reaction kinetics through isomerization cases with the basis of density - functional calculations",	1%

	Biochemistry and Molecular Biology Education, 2020 Publication	
6	assets.researchsquare.com Internet Source	1 %
7	escholarship.org Internet Source	1 %
8	fti.itb.ac.id Internet Source	1 %
9	Tran Dieu Hang, Huynh Minh Hung, Minh Tho Nguyen. " Comparative Study of Methanol Activation by Different Small Mixed Silicon Clusters Si M with M = H, Li, Na, Cu, and Ag ", ACS Omega, 2017 Publication	1 %
10	Nicolas Louis, Stephan Kohaut, Michael Springborg. "$$\hbox {Ag}_{m} \hbox {Rh}_n$$ clusters with $$m+n\le 55$$", Theoretical Chemistry Accounts, 2021 Publication	<1 %
11	repositori.upf.edu Internet Source	<1 %
12	web.archive.org Internet Source	<1 %
13	www.mdpi.com Internet Source	<1 %

14	Density Functional Theory in Quantum Chemistry, 2014. Publication	<1 %
15	Narbe Mardirossian, Martin Head-Gordon. "How Accurate Are the Minnesota Density Functionals for Noncovalent Interactions, Isomerization Energies, Thermochemistry, and Barrier Heights Involving Molecules Composed of Main-Group Elements?", Journal of Chemical Theory and Computation, 2016 Publication	<1 %
16	Rizka N. Fadilla, Febdian Rusydi, Nufida D. Aisyah, Vera Khoirunisa et al. "A Density-Functional Study of the Conformational Preference of Acetylcholine in the Neutral Hydrolysis", Molecules, 2020 Publication	<1 %
17	Trouillas, P.. "A DFT study of the reactivity of OH groups in quercetin and taxifolin antioxidants: The specificity of the 3-OH site", Food Chemistry, 200608 Publication	<1 %
18	www.pubfacts.com Internet Source	<1 %
19	pubs.rsc.org Internet Source	<1 %

20	Dragan Amić, Višnja Stepanić, Bono Lučić, Zoran Marković, Jasmina M. Dimitrić Marković. "PM6 study of free radical scavenging mechanisms of flavonoids: why does O–H bond dissociation enthalpy effectively represent free radical scavenging activity?", Journal of Molecular Modeling, 2013 Publication	<1 %
21	Ioannis Galanis, Iraklis Anagnostopoulos, Priyaa Gurunathan, Dona Burkard. "Environmental-Based Speed Recommendation for Future Smart Cars", Future Internet, 2019 Publication	<1 %
22	Quantum Modeling of Complex Molecular Systems, 2015. Publication	<1 %
23	pure.rug.nl Internet Source	<1 %
24	C. Gharbi, Y. Ajili, D. Ben Abdallah, M. Hochlaf. "Sodium isocyanide–Helium potential energy surface and astrophysical applications", Theoretical Chemistry Accounts, 2021 Publication	<1 %
25	www.koreascience.or.kr Internet Source	<1 %

26	"Kinetics and Dynamics", Springer Science and Business Media LLC, 2010 Publication	<1 %
27	Olga V. Kushch, Iryna O. Hordieieva, Mykhailo O. Kompanets, Olha O. Zosenko, Iosip A. Opeida, Alexander N. Shendrik. " Hydrogen Atom Transfer from Benzyl Alcohols to -Oxyl Radicals. Reactivity Parameters ", The Journal of Organic Chemistry, 2021 Publication	<1 %
28	Salamun, Fatimah, Ahmad Fauzi, Seling N. Praduwana, Ni'matuzahroh. " Larvicidal toxicity and parasporal inclusion of native BK5.2 against ", Journal of Basic and Clinical Physiology and Pharmacology, 2021 Publication	<1 %
29	Tianshu Du, Frank H. Quina, Daniel Tunega, Jianyu Zhang, Adelia J. A. Aquino. "Theoretical O–CH3 bond dissociation enthalpies of selected aromatic and non-aromatic molecules", Theoretical Chemistry Accounts, 2020 Publication	<1 %
30	hdl.handle.net Internet Source	<1 %
31	www.science.gov Internet Source	<1 %

32	www.scribd.com Internet Source	<1%
33	Ousman Boukar, Jean Jules Fifen, Mama Nsangou, Hassen Ghalila, Jeanet Conradie. "Structures and relative stabilities of hydrated ferrous ion clusters and temperature effects", New Journal of Chemistry, 2021 Publication	<1%
34	Xue Li, Yanyan Zhu, Chunmei Liu, Xincheng Lin, Wenjing Zhang, Mingsheng Tang. "Molecular recognition of cyclodecapeptides to ibuprofen and naproxen enantiomers: a theoretical study", Structural Chemistry, 2017 Publication	<1%
35	Yong-Quan Qu, Yong Wang, Jing Li, Ke-Li Han. "Quantum chemical study of surface reactions of glycine on the Si(100)-2×1 surface", Surface Science, 2004 Publication	<1%

Exclude quotes	Off	Exclude matches	Off
Exclude bibliography	On		

O—H and C—H bond dissociations in non-phenyl and phenyl groups: A DFT study with dispersion and long-range corrections

GRADEMARK REPORT

FINAL GRADE

/0

GENERAL COMMENTS

Instructor

PAGE 1

PAGE 2

PAGE 3

PAGE 4

PAGE 5

PAGE 6

PAGE 7

PAGE 8

PAGE 9